

4

Dynamics of Excitable Cells

Michael R. Guevara

4.1 Introduction

In this chapter, we describe a preparation – the giant axon of the squid – that was instrumental in allowing the ionic basis of the action potential to be elucidated. We also provide an introduction to the voltage-clamp technique, the application of which to the squid axon culminated in the Hodgkin–Huxley equations, which we introduce. Hodgkin and Huxley were awarded the Nobel Prize in Physiology or Medicine in 1963 for this work. We also provide a brief introduction to the FitzHugh–Nagumo equations, a reduced form of the Hodgkin–Huxley equations.

4.2 The Giant Axon of the Squid

4.2.1 Anatomy of the Giant Axon of the Squid

The **giant axon of the squid** is one of a pair of axons that runs down the length of the mantle of the squid in the stellate nerve (Figure 4.1). When the squid wishes to move quickly (e.g., to avoid a predator), it sends between one and eight action potentials down each of these axons to initiate contraction of the muscles in its mantle. This causes a jet of water to be squirted out, and the animal is suddenly propelled in the opposite direction. The conduction velocity of the action potentials in this axon is very high (on the order of 20 m/s), which is what one might expect for an escape mechanism. This high conduction velocity is largely due to the fact that the axon has a large diameter, a large cross-sectional area, and thus a low resistance to the longitudinal flow of current in its cytoplasm. The description of this large axon by Young in 1936 is the anatomical discovery that permitted the use of this axon in the pioneering electrophysiological work of Cole, Curtis, Marmont, Hodgkin, and Huxley in the 1940s and 1950s (see references in Cole 1968; Hodgkin 1964). The common North Atlantic squid (*Loligo pealei*) is used in North America.

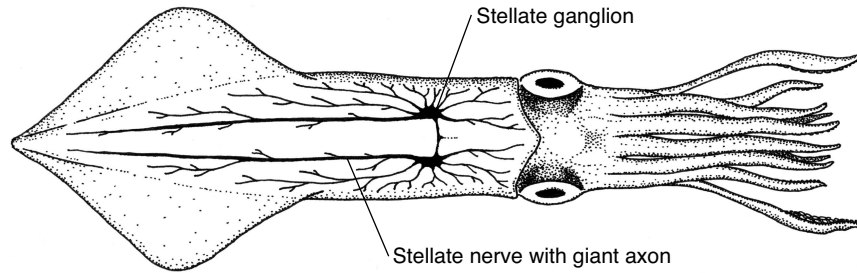


Figure 4.1. Anatomical location of the giant axon of the squid. Drawing by Tom Inoué.

4.2.2 Measurement of the Transmembrane Potential

The large diameter of the axon (as large as $1000\ \mu\text{m}$) makes it possible to insert an axial electrode directly into the axon (Figure 4.2A). By placing another electrode in the fluid in the bath outside of the axon (Figure 4.2B), the voltage difference across the axonal membrane (the **transmembrane potential** or **transmembrane voltage**) can be measured. One can also stimulate the axon to fire by injecting a current pulse with another set of extracellular electrodes (Figure 4.2B), producing an action potential that will propagate down the axon. This action potential can then be recorded with the intracellular electrode (Figure 4.2C). Note the afterhyperpolarization following the action potential. One can even roll the cytoplasm out of the axon, cannulate the axon, and replace the cytoplasm with fluid of a known composition (Figure 4.3). When the fluid has an ionic composition close enough to that of the cytoplasm, the action potential resembles that recorded in the intact axon (Figure 4.2D). The cannulated, internally perfused axon is the basic preparation that allowed electrophysiologists to sort out the ionic basis of the action potential fifty years ago.

The advantage of the large size of the invertebrate axon is appreciated when one contrasts it with a mammalian neuron from the central nervous system (Figure 4.4). These neurons have axons that are very small; indeed, the soma of the neuron in Figure 4.4, which is much larger than the axon, is only on the order of $10\ \mu\text{m}$ in diameter.

4.3 Basic Electrophysiology

4.3.1 Ionic Basis of the Action Potential

Figure 4.5 shows an action potential in the Hodgkin–Huxley model of the squid axon. This is a four-dimensional system of ordinary differential equa-

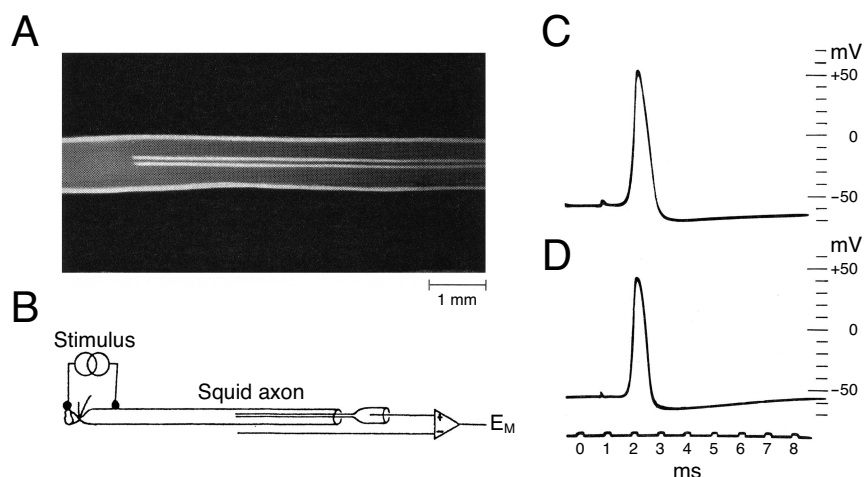


Figure 4.2. (A) Giant axon of the squid with internal electrode. Panel A from Hodgkin and Keynes (1956). (B) Axon with intracellularly placed electrode, ground electrode, and pair of stimulus electrodes. Panel B from Hille (2001). (C) Action potential recorded from intact axon. Panel C from Baker, Hodgkin, and Shaw (1961). (D) Action potential recorded from perfused axon. Panel D from Baker, Hodgkin, and Shaw (1961).

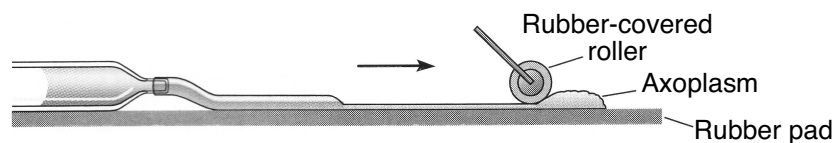


Figure 4.3. Cannulated, perfused giant axon of the squid. From Nicholls, Martin, Wallace, and Fuchs (2001).

tions that describes the three main currents underlying the action potential in the squid axon. Figure 4.5 also shows the time course of the conductance of the two major currents during the action potential. The fast inward sodium current (I_{Na}) is the current responsible for generating the upstroke of the action potential, while the potassium current (I_K) repolarizes the membrane. The leakage current (I_L), which is not shown in Figure 4.5, is much smaller than the two other currents. One should be aware that other neurons can have many more currents than the three used in the classic Hodgkin–Huxley description.

4.3.2 Single-Channel Recording

The two major currents mentioned above (I_{Na} and I_K) are currents that pass across the cellular membrane through two different types of channels

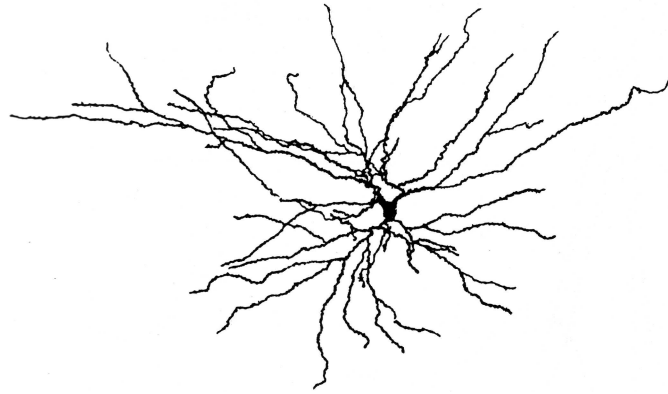


Figure 4.4. Stellate cell from rat thalamus. From Alonso and Klink (1993).

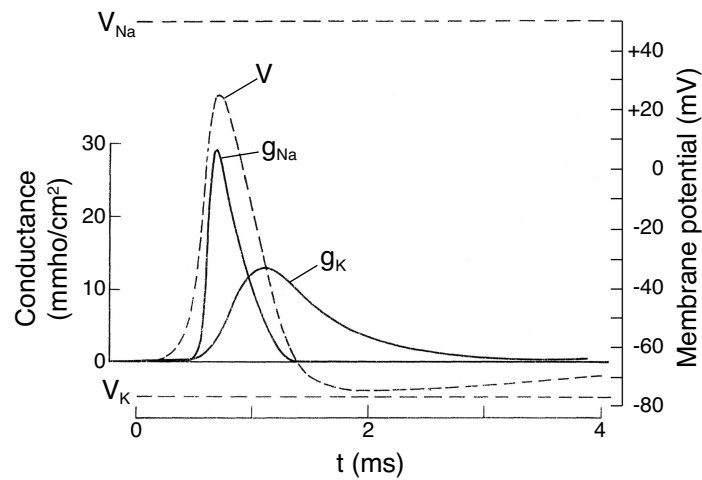


Figure 4.5. Action potential from Hodgkin–Huxley model and the conductances of the two major currents underlying the action potential in the model. Adapted from Hodgkin (1958).

lying in the membrane. The sodium channel is highly selective for sodium, while the potassium channel is highly selective for potassium. In addition, the manner in which these channels are controlled by the transmembrane potential is very different, as we shall see later. Perhaps the most direct evidence for the existence of single channels in the membranes of cells comes from the patch-clamp technique (for which the Nobel prize in Physiology or Medicine was awarded to Neher and Sakmann in 1991). In this technique, a glass microelectrode with tip diameter on the order of $1 \mu\text{m}$ is brought up against the membrane of a cell. If one is lucky, there will be only one channel in the patch of membrane subtended by the rim of the electrode,

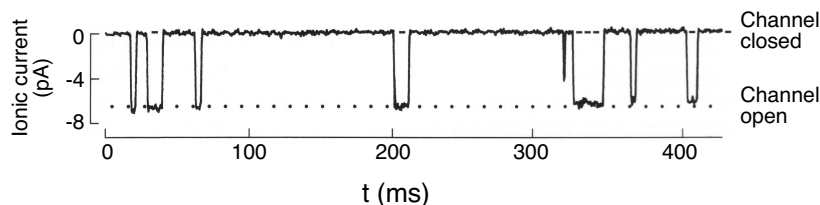


Figure 4.6. A single-channel recording using the patch-clamp technique. From Sánchez, Dani, Siemen, and Hille (1986).

and one will pick up a signal similar to that shown in Figure 4.6. The channel opens and closes in an apparently random fashion, allowing a fixed amount of current (on the order of picoamperes) to flow through it when it is in the open state.

4.3.3 The Nernst Potential

The concentrations of the major ions inside and outside the cell are very different. For example, the concentration of K^+ is much higher inside the squid axon than outside of it (400 mM versus 20 mM), while the reverse is true of Na^+ (50 mM versus 440 mM). These concentration gradients are set up by the sodium–potassium pump, which works tirelessly to pump sodium out of the cell and potassium into it.

A major consequence of the existence of the K^+ gradient is that the resting potential of the cell is negative. To understand this, one needs to know that the cell membrane is very permeable to K^+ at rest, and relatively impermeable to Na^+ . Consider the thought experiment in Figure 4.7. One has a bath that is divided into two chambers by a semipermeable membrane that is very permeable to the cation K^+ but impermeable to the anion A^- . One then adds a high concentration of the salt KA into the water in the left-hand chamber, and a much lower concentration to the right-hand chamber (Figure 4.7A). There will immediately be a diffusion of K^+ ions through the membrane from left to right, driven by the concentration gradient. However, these ions will build up on the right, tending to electrically repel other K^+ ions wanting to diffuse from the left. Eventually, one will end up in electrochemical equilibrium (Figure 4.7B), with the voltage across the membrane in the steady state being given by the Nernst or equilibrium potential E_K ,

$$E_K = \frac{RT}{zF} \ln \left(\frac{[K^+]_o}{[K^+]_i} \right), \quad (4.1)$$

where $[K^+]_o$ and $[K^+]_i$ are the external and internal concentrations of K^+ respectively, R is the Rydberg gas constant, T is the temperature in degrees Kelvin, z is the charge on the ion (+1 for K^+), and F is Faraday's constant.

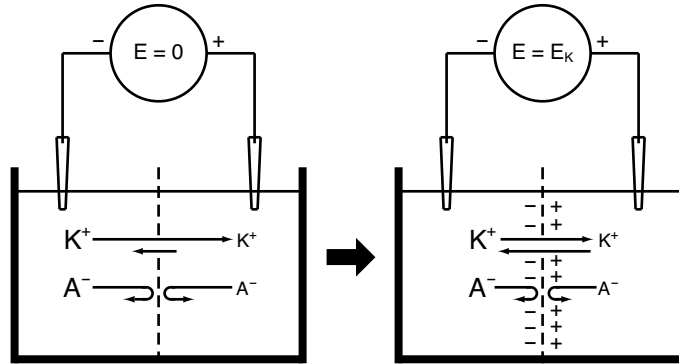


Figure 4.7. Origin of the Nernst potential.

4.3.4 A Linear Membrane

Figure 4.8A shows a membrane with potassium channels inserted into it. The membrane is a lipid bilayer with a very high resistance. Let us assume that the density of the channels in the membrane, their single-channel conductance, and their mean open time are such that they have a conductance of g_K millisiemens per square centimeter (mS cm^{-2}). The current through these channels will then be given by

$$I_K = g_K(V - E_K). \quad (4.2)$$

There will thus be zero current flow when the transmembrane potential is at the Nernst potential, an inward flow of current when the transmembrane potential is negative with respect to the Nernst potential, and an outward flow of current when the transmembrane potential is positive with respect to the Nernst potential (consider Figure 4.7B to try to understand why this should be so). (An inward current occurs when there is a flow of positive ions into the cell or a flow of negative ions out of the cell.) The electrical equivalent circuit for equation (4.2) is given by the right-hand branch of the circuit in Figure 4.8B.

Now consider the dynamics of the membrane potential when it is not at its equilibrium value. When the voltage is changing, there will be a flow of current through the capacitive branch of the circuit of Figure 4.8B. The capacitance is due to the fact that the membrane is an insulator (since it is largely made up of lipids), and is surrounded on both sides by conducting fluid (the cytoplasm and the interstitial fluid). The equation of state of a capacitor is

$$Q = -CV, \quad (4.3)$$

where Q is the charge on the capacitance, C is the capacitance, and V is the voltage across the capacitance. Differentiating both sides of this expression

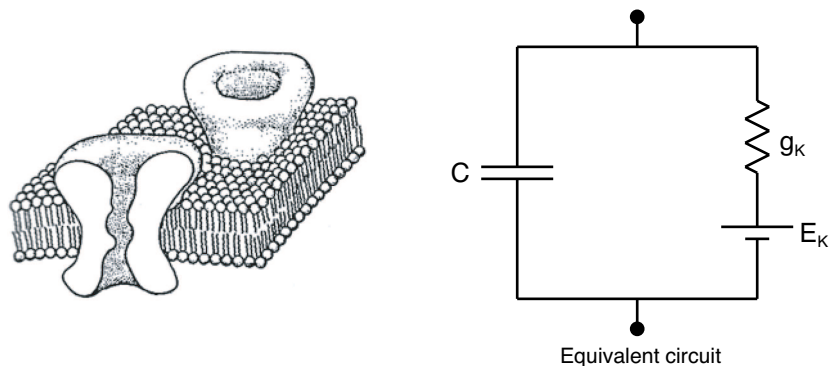


Figure 4.8. (A) Schematic view of potassium channels inserted into lipid bilayer. Panel A from Hille (2001). (B) Electrical equivalent circuit of membrane and channels.

with respect to time t , one obtains

$$\frac{dV}{dt} = -\frac{I_K}{C} = -\frac{g_K}{C}(V - E_K) = -\frac{V - E_K}{\tau}, \quad (4.4)$$

where $\tau = C/g_K = R_K C$ is the **time constant** of the membrane. Here, we have also used the definition of current $I = dQ/dt$. The solution of this one-dimensional linear ordinary differential equation is

$$V(t) = E_K - (E_K - V(0))e^{-t/\tau}. \quad (4.5)$$

Unfortunately, the potassium current I_K is not as simple as that postulated in equation (4.2). This is because we have assumed that the probability of the channel being open is a constant that is independent of time and voltage, and thus g_K is not a function of voltage and time. This is not the case, as we shall see next.

4.4 Voltage-Clamping

4.4.1 The Voltage-Clamp Technique

While the large size of the squid axon was invaluable in allowing the transmembrane potential to be easily measured, it was really the use of this preparation in conjunction with the invention of the voltage-clamp technique that revolutionized the field. The voltage-clamp technique was pioneered by Cole, Curtis, Hodgkin, Huxley, Katz, and Marmont following the hiatus provided by the Second World War (see references in Cole 1968; Hodgkin 1964). Voltage-clamping involves placing two internal electrodes: one to measure the transmembrane potential as before, and the other to inject current (Figure 4.9). Using electronic feedback circuitry, one then

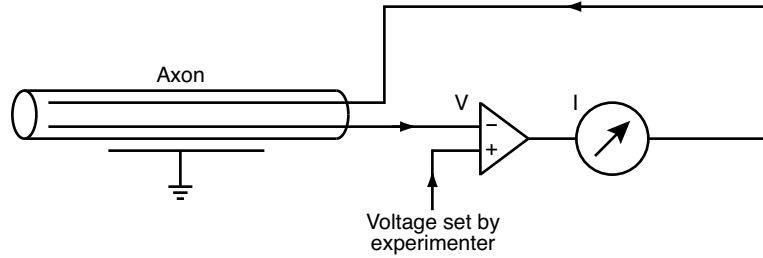


Figure 4.9. Schematic diagram illustrating voltage-clamp technique.

injects current so that a predetermined fixed voltage is maintained across the membrane. The current injected by the circuitry is then the mirror image of the current generated by the cell membrane at that potential. In addition, the effective length of the preparation is kept sufficiently short so that effects due to intracellular spread of current are mitigated: One thus transforms a problem inherently described by a partial differential equation into one reasonably well described by an ordinary differential equation.

4.4.2 A Voltage-Clamp Experiment

Figure 4.10B shows the clamp current during a voltage-clamp step from -65 mV to -9 mV (Figure 4.10A). This current can be broken down into the sum of four different currents: a capacitative current (Figure 4.10C), a leakage current (Figure 4.10C), a sodium current (Figure 4.10D), and a potassium current (Figure 4.10E). The potassium current turns on (**activates**) relatively slowly. In contrast, the sodium current activates very quickly. In addition, unlike the potassium current, the sodium current then turns off (**inactivates**), despite the fact that the voltage or transmembrane potential, V , is held constant.

4.4.3 Separation of the Various Ionic Currents

How do we know that the trace of Figure 4.10B is actually composed of the individual currents shown in the traces below it? This conclusion is based largely on three different classes of experiments involving ion substitution, specific blockers, and specific clamp protocols. Figure 4.11B shows the clamp current in response to a step from -65 mV to -9 mV (Figure 4.11A). Also shown is the current when all but 10% of external Na^+ is replaced with an impermeant ion. The difference current (Figure 4.11C) is thus essentially the sodium current. Following addition of tetrodotoxin, a specific blocker of the sodium current, only the outward I_K component remains, while following addition of tetraethylammonium, which blocks potassium channels, only the inward I_{Na} component remains.

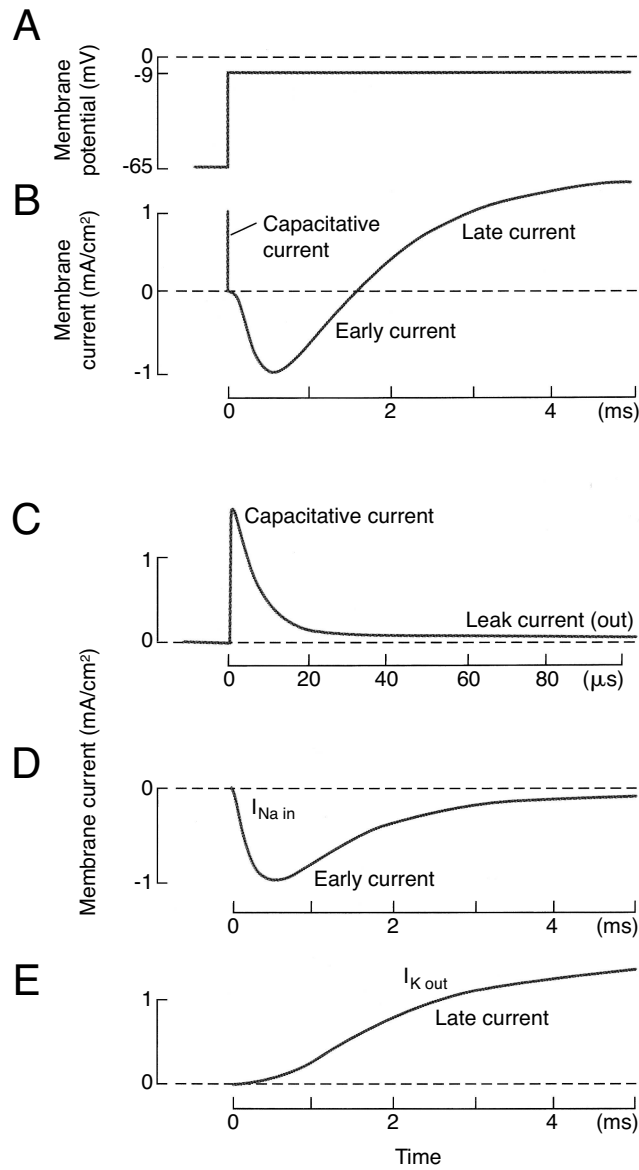


Figure 4.10. Voltage-clamp experiment on squid axon. From Nicholls, Martin, Wallace, and Fuchs (2001).

4.5 The Hodgkin–Huxley Formalism

4.5.1 Single-Channel Recording of the Potassium Current

Figure 4.12A shows a collection of repeated trials in which the voltage is clamped from -100 mV to $+50$ mV. The potassium channel in the

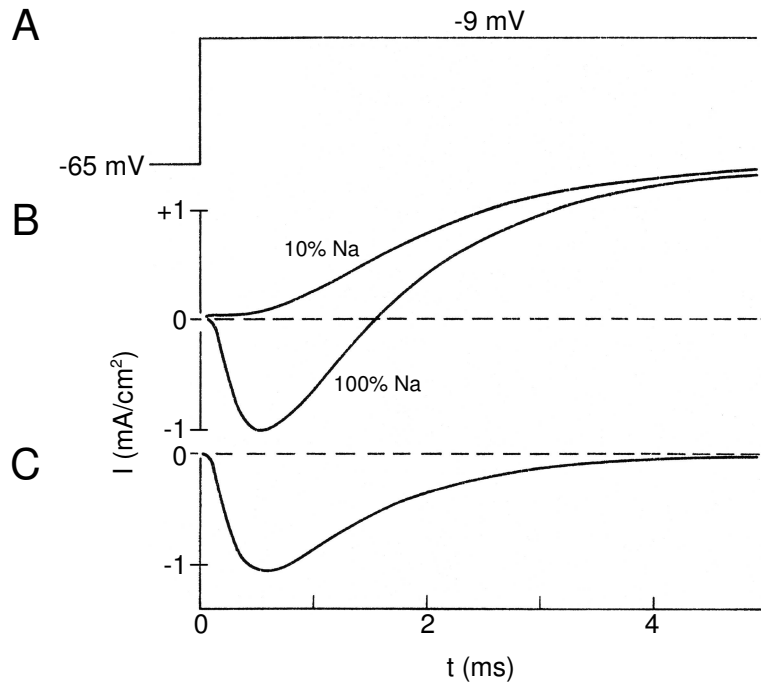


Figure 4.11. Effect of removal of extracellular sodium on voltage-clamp record. Adapted from Hodgkin (1958).

patch opens after a variable delay and then tends to stay open. Thus, the ensemble-averaged trace (Figure 4.12B) has a sigmoidal time course similar to the macroscopic current recorded in the axon (e.g., Figure 4.10E). It is thus clear that the macroscopic concept of the time course of activation is connected with the microscopic concept of the latency to first opening of a channel.

4.5.2 Kinetics of the Potassium Current I_K

The equation developed by Hodgkin and Huxley to describe the potassium current, I_K , is

$$I_K(V, t) = g_K(V - E_K) = \bar{g}_K [n(V, t)]^4 (V - E_K), \quad (4.6)$$

where \bar{g}_K is the maximal conductance, and where n is a “gating” variable satisfying

$$\frac{dn}{dt} = \alpha_n(1 - n) - \beta_n n.$$

Let us try to understand where this equation comes from.

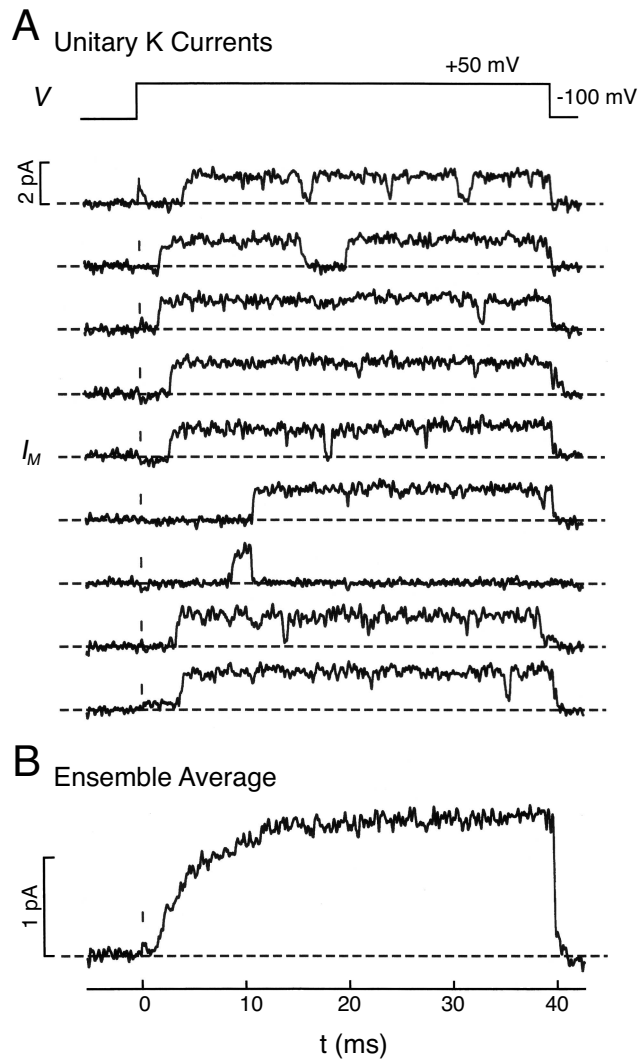


Figure 4.12. (A) Repeated voltage-clamp trials in single-channel recording mode for I_K . (B) Ensemble average of above recordings. Figure from F. Bezanilla.

Assume that there is one gate (the “ n -gate”) controlling the opening and closing of the potassium channel. Also assume that it follows a first-order reaction scheme



where the rate constants α_n and β_n , which are functions of voltage (but are constant at any given voltage), control the transitions between the closed

(*C*) and open (*O*) states of the gate. The variable n can then be interpreted as the fraction of gates that are open, or, equivalently, as the probability that a given gate will be open. One then has

$$\frac{dn}{dt} = \alpha_n(1 - n) - \beta_n n = \frac{n_\infty - n}{\tau_n}, \quad (4.8)$$

where

$$\begin{aligned} n_\infty &= \frac{\alpha_n}{\alpha_n + \beta_n}, \\ \tau_n &= \frac{1}{\alpha_n + \beta_n}. \end{aligned} \quad (4.9)$$

The solution of the ordinary differential equation in (4.8), when V is constant, is

$$n(t) = n_\infty - (n_\infty - n(0))e^{-t/\tau_n}. \quad (4.10)$$

The formula for I_K would then be

$$I_K = \bar{g}_K n(V - E_K), \quad (4.11)$$

with

$$\frac{dn}{dt} = \frac{n_\infty - n}{\tau_n}, \quad (4.12)$$

where \bar{g}_K is the maximal conductance. However, Figure 4.13A shows that g_K has a waveform that is not simply an exponential rise, being more sigmoidal in shape. Hodgkin and Huxley thus took n to the fourth power in equation (4.11), resulting in

$$I_K = \bar{g}_K n^4(V - E_K) = g_K(V - E_K). \quad (4.13)$$

Figure 4.13B shows the n_∞ and τ_n curves, while Figure 4.14 shows the calculated time courses of n and n^4 during a voltage-clamp step.

4.5.3 Single-Channel Recording of the Sodium Current

Figure 4.15A shows individual recordings from repeated clamp steps from -80 mV to -40 mV in a patch containing more than one sodium channel. Note that there is a variable latency to the first opening of a channel, which accounts for the time-dependent activation in the ensemble-averaged recording (Figure 4.15B). The inactivation seen in the ensemble-averaged recording is traceable to the fact that channels close, and eventually stay closed, in the patch-clamp recording.

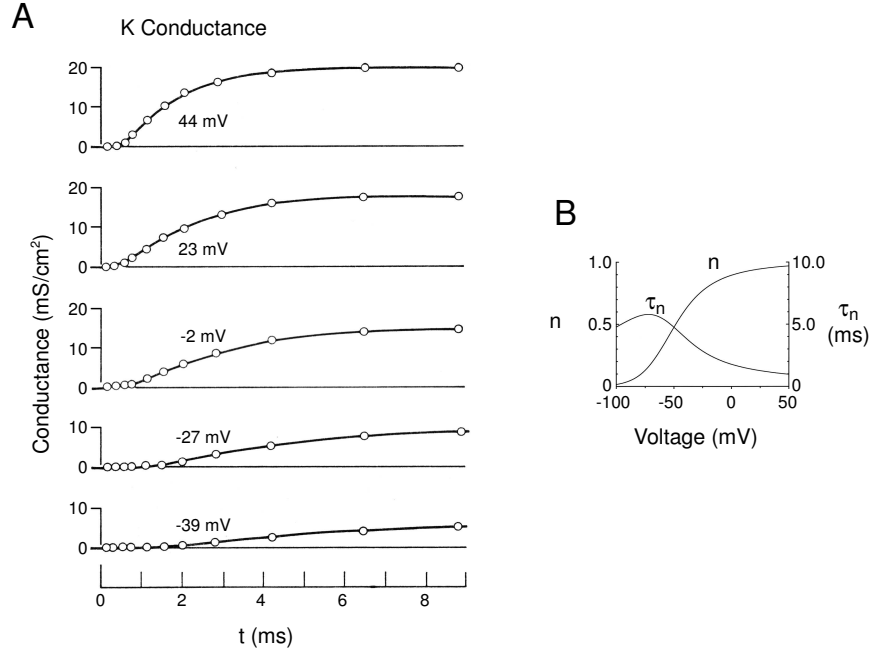


Figure 4.13. (A) Circles are data points for g_K calculated from experimental values of I_K , V , and E_K using equation (4.13). The curves are the fit using the Hodgkin–Huxley formalism. Panel A from Hodgkin (1958). (B) n_∞ and τ_n as functions of V .

4.5.4 Kinetics of the Sodium Current I_{Na}

Again, fitting of the macroscopic currents led Hodgkin and Huxley to the following equation for the sodium current, I_{Na} ,

$$I_{Na} = \bar{g}_{Na} m^3 h (V - E_{Na}) = g_{Na} (V - E_{Na}), \quad (4.14)$$

where m is the **activation** variable, and h is the **inactivation** variable. This implies that

$$g_{Na}(V, t) = \bar{g}_{Na} [m(V, t)]^3 h(V, t) = \frac{I_{Na}(V, t)}{(V - E_{Na})}. \quad (4.15)$$

Figure 4.16A shows that this equation fits the g_{Na} data points very well.

The equations directing the movement of the m -gate are very similar to those controlling the n -gate. Again, one assumes a kinetic scheme of the form



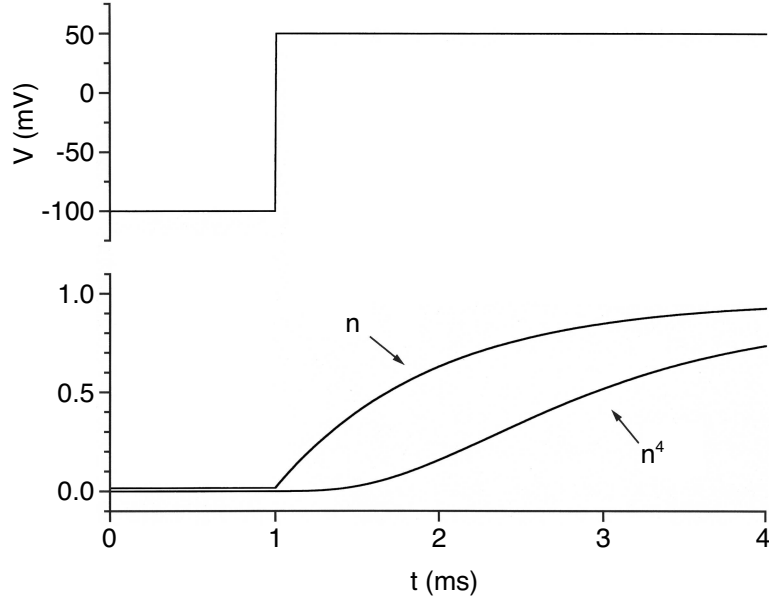


Figure 4.14. Time course of n and n^4 in the Hodgkin–Huxley model.

where the rate constants α_m and β_m are functions of voltage, but are constant at any given voltage. Thus m satisfies

$$\frac{dm}{dt} = \alpha_m(1 - m) - \beta_m m = \frac{m_\infty - m}{\tau_m}, \quad (4.17)$$

where

$$\begin{aligned} m_\infty &= \frac{\alpha_m}{\alpha_m + \beta_m}, \\ \tau_m &= \frac{1}{\alpha_m + \beta_m}. \end{aligned} \quad (4.18)$$

The solution of equation (4.17) when V is constant is

$$m(t) = m_\infty - (m_\infty - m(0))e^{-t/\tau_m}. \quad (4.19)$$

Similarly, one has for the h -gate

$$C \frac{\alpha_h}{\beta_h} O, \quad (4.20)$$

where the rate constants α_h and β_h are functions of voltage, but are constant at any given voltage. Thus h satisfies

$$\frac{dh}{dt} = \alpha_h(1 - h) - \beta_h h = \frac{h_\infty - h}{\tau_h}, \quad (4.21)$$

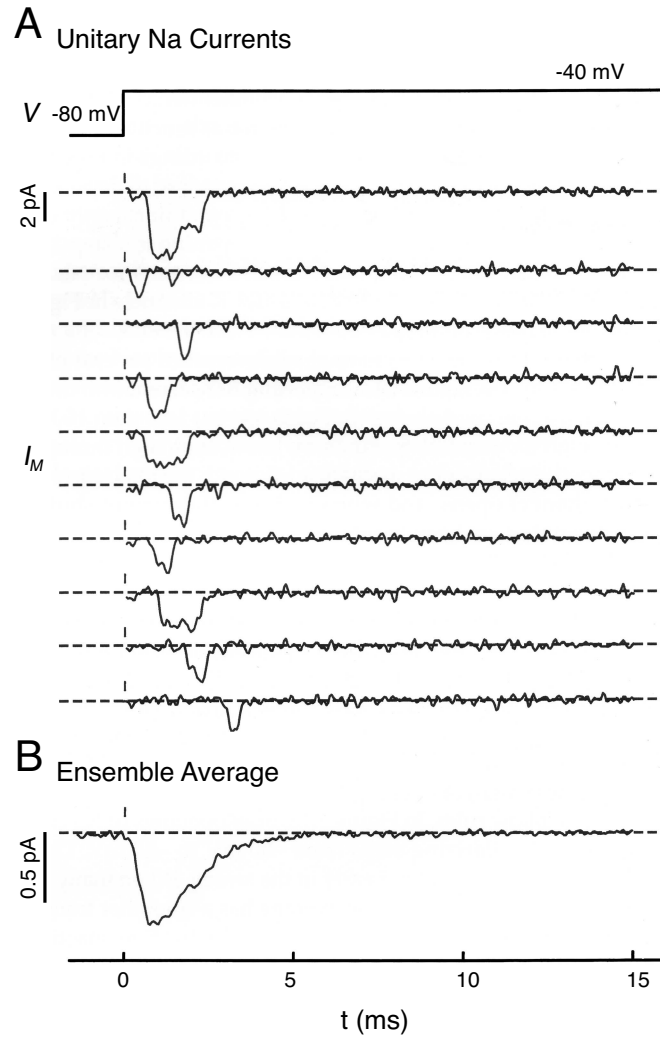


Figure 4.15. (A) Repeated voltage-clamp trials in single-channel recording mode for I_{Na} . (B) Ensemble average of above recordings. Figure from J.B. Patlak.

where

$$\begin{aligned}
 h_{\infty} &= \frac{\alpha_h}{\alpha_h + \beta_h}, \\
 \tau_h &= \frac{1}{\alpha_h + \beta_h}.
 \end{aligned}
 \tag{4.22}$$

The solution of equation (4.21) when V is constant is

$$h(t) = h_{\infty} - (h_{\infty} - h(0))e^{-t/\tau_h}.
 \tag{4.23}$$

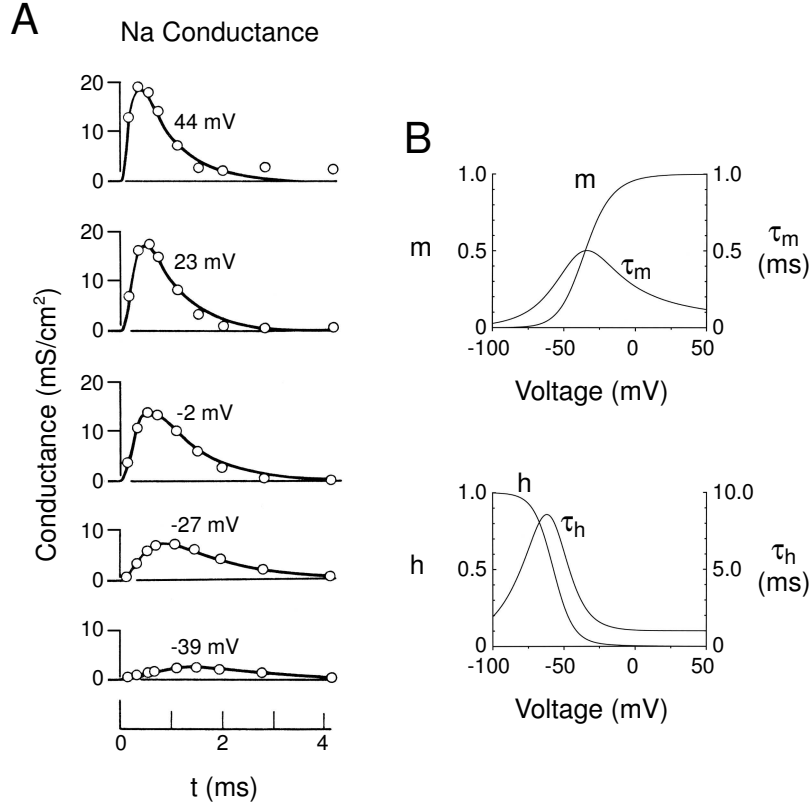


Figure 4.16. (A) Circles are data points for g_{Na} calculated from experimental values of I_{Na} , V , and E_{Na} using equation (4.15). The curves are the fit produced by the Hodgkin–Huxley formalism. Panel A from Hodgkin (1958). (B) m_∞ , τ_m , h_∞ , and τ_h as functions of voltage.

The general formula for I_{Na} is thus

$$I_{\text{Na}} = \bar{g}_{\text{Na}} m^3 h (V - E_{\text{Na}}), \quad (4.24)$$

with m satisfying equation (4.17) and h satisfying equation (4.21). Figure 4.16B shows m_∞ , τ_m , h_∞ , and τ_h , while Figure 4.17 shows the evolution of m , m^3 , h , and $m^3 h$ during a voltage-clamp step.

4.5.5 The Hodgkin–Huxley Equations

Putting together all the equations above, one obtains the Hodgkin–Huxley equations appropriate to the standard squid temperature of 6.3 degrees Celsius (Hodgkin and Huxley 1952). This is a system of four coupled nonlinear

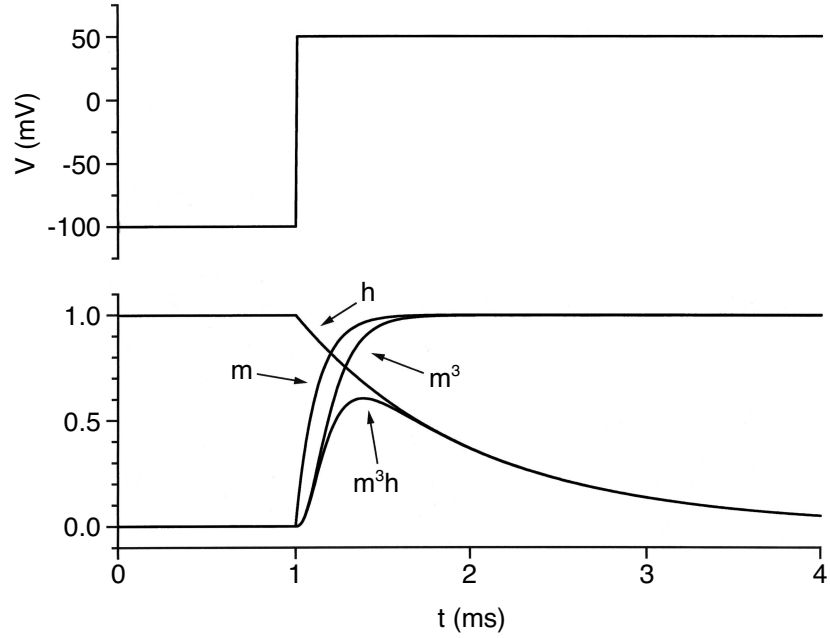


Figure 4.17. Time course of m , m^3 , h , and m^3h in the Hodgkin–Huxley model.

ordinary differential equations,

$$\begin{aligned} \frac{dV}{dt} &= -\frac{1}{C} [(\bar{g}_{\text{Na}} m^3 h (V - E_{\text{Na}}) + \bar{g}_{\text{K}} n^4 (V - E_{\text{K}}) \\ &\quad + \bar{g}_{\text{L}} (V - E_{\text{L}}) + I_{\text{stim}}], \\ \frac{dm}{dt} &= \alpha_m (1 - m) - \beta_m m, \\ \frac{dh}{dt} &= \alpha_h (1 - h) - \beta_h h, \\ \frac{dn}{dt} &= \alpha_n (1 - n) - \beta_n n, \end{aligned} \quad (4.25)$$

where

$$\bar{g}_{\text{Na}} = 120 \text{ mS cm}^{-2}, \quad \bar{g}_{\text{K}} = 36 \text{ mS cm}^{-2}, \quad \bar{g}_{\text{L}} = 0.3 \text{ mS cm}^{-2},$$

and

$$E_{\text{Na}} = +55 \text{ mV}, \quad E_{\text{K}} = -72 \text{ mV}, \quad E_{\text{L}} = -49.387 \text{ mV}, \quad C = 1 \text{ } \mu\text{F cm}^{-2}.$$

Here I_{stim} is the total stimulus current, which might be a periodic pulse train or a constant (“bias”) current. The voltage-dependent rate constants

are given by

$$\begin{aligned}
 \alpha_m &= 0.1(V + 35)/(1 - \exp(-(V + 35)/10)), \\
 \beta_m &= 4 \exp(-(V + 60)/18), \\
 \alpha_h &= 0.07 \exp(-(V + 60)/20), \\
 \beta_h &= 1/(\exp(-(V + 30)/10) + 1), \\
 \alpha_n &= 0.01(V + 50)/(1 - \exp(-(V + 50)/10)), \\
 \beta_n &= 0.125 \exp(-(V + 60)/80).
 \end{aligned}
 \tag{4.26}$$

Note that these equations are not the same as in the original papers of Hodgkin and Huxley, since the modern-day convention of the inside of the membrane being negative to the outside of membrane during rest is used above, and the voltage is the actual transmembrane potential, not its deviation from the resting potential.

Figure 4.18 shows m , h , and n during the action potential. It is clear that I_{Na} activates more quickly than I_{K} , which is a consequence of τ_m being smaller than τ_n (see Figures 4.13B and 4.16B).

4.5.6 The FitzHugh–Nagumo Equations

The full Hodgkin–Huxley equations are a four-dimensional system of ordinary differential equations. It is thus difficult to obtain a visual picture of trajectories in this system. In the 1940s, Bonhoeffer, who had been conducting experiments on the passivated iron wire analogue of nerve conduction, realized that one could think of basic electrophysiological properties such as excitability, refractoriness, accommodation, and automaticity in terms of a simple two-dimensional system that had a phase portrait very similar to the van der Pol oscillator (see, e.g., Figures 8 and 9 in Bonhoeffer 1948). Later, FitzHugh wrote down a modified form of the van der Pol equations to approximate Bonhoeffer’s system, calling these equations the Bonhoeffer–van der Pol equations (FitzHugh 1961). FitzHugh also realized that in the Hodgkin–Huxley equations, the variables V and m tracked each other during an action potential, so that one could be expressed as an algebraic function of the other (this also holds true for h and n). At about the same time as this work of FitzHugh, Nagumo et al. were working on electronic analogues of nerve transmission, and came up with essentially the same equations. These equations thus tend to be currently known as the FitzHugh–Nagumo equations and are given by

$$\begin{aligned}
 \frac{dx}{dt} &= c \left(x - \frac{x^3}{3} + y + S(t) \right), \\
 \frac{dy}{dt} &= -\frac{(x - a + by)}{c},
 \end{aligned}
 \tag{4.27}$$

where x is a variable (replacing variables V and m in the Hodgkin–Huxley system) representing transmembrane potential and excitability, while y is

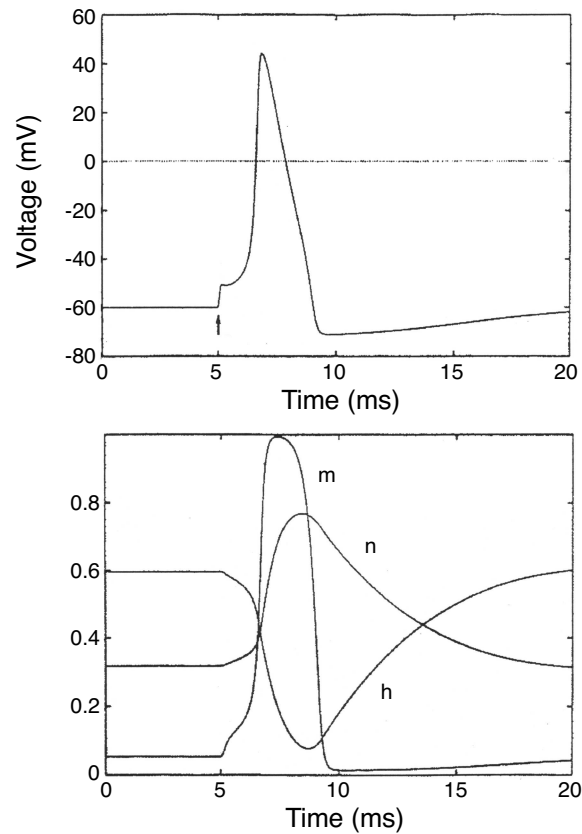


Figure 4.18. Time course of m , h , and n in the Hodgkin–Huxley model during an action potential.

a variable (replacing variables h and n in the Hodgkin–Huxley system) responsible for refractoriness and accommodation. The function $S(t)$ is the stimulus, and a , b , and c are parameters. The computer exercises in Section 4.8 explore the properties of the FitzHugh–Nagumo system in considerable detail.

4.6 Conclusions

The Hodgkin–Huxley model has been a great success, replicating many of the basic electrophysiological properties of the squid axon, e.g., excitability, refractoriness, and conduction speed. However, there are several discrepancies between experiment and model: For example injection of a constant bias current in the squid axon does not lead to spontaneous firing, as it does

in the equations. This has led to updated versions of the Hodgkin–Huxley model being produced to account for these discrepancies (e.g., Clay 1998).

4.7 Computer Exercises: A Numerical Study on the Hodgkin–Huxley Equations

We will use the Hodgkin–Huxley equations to explore annihilation and triggering of limit-cycle oscillations, the existence of two resting potentials, and other phenomena associated with bifurcations of fixed points and limit cycles (see Chapter 3).

The Hodgkin–Huxley model, given in equation (4.25), consists of a four-dimensional set of ordinary differential equations, with variables V, m, h, n . The XPP file **hh.ode** contains the Hodgkin–Huxley equations.* The variable V represents the transmembrane potential, which is generated by the sodium current (**curna** in **hh.ode**), the potassium current (**curk**), and a leak current (**curleak**). The variables m and h , together with V , control the sodium current. The potassium current is controlled by the variables n and V . The leak current depends only on V .

Ex. 4.7-1. Annihilation and Triggering in the Hodgkin–Huxley Equations.

We shall show that one can annihilate bias-current induced firing in the Hodgkin–Huxley (Hodgkin and Huxley 1952) equations by injecting a single well-timed stimulus pulse (Guttman, Lewis, and Rinzel 1980). Once activity is so abolished, it can be restarted by injecting a strong enough stimulus pulse.

- (a) **Nature of the Fixed Point.** We first examine the response of the system to a small perturbation, using direct numerical integration of the system equations. We will inject a small stimulus pulse to deflect the state point away from its normal location at the fixed point. The way in which the trajectory returns to the fixed point will give us a clue as to the nature of the fixed point (i.e., node, focus, saddle, etc.). We will then calculate eigenvalues of the point to confirm our suspicions.

Start up XPP using the source file **hh.ode**.

The initial conditions in **hh.ode** have been chosen to correspond to the fixed point of the system when no stimulation is applied. This can be verified by integrating the equations numerically

*See Introduction to XPP in Appendix A.

(select `Initialconds` and then `Go` from the main `XPP` window). Note that the transmembrane potential (V) rests at -60 mV, which is termed the **resting potential**.

Let us now investigate the effect of injecting a stimulus pulse. Click on the `Param` button at the top of the main `XPP` window. In the `Parameters` window that pops up, the parameters `tstart`, `duration`, and `amplitude` control the time at which the current-pulse stimulus is turned on, the duration of the pulse, and the amplitude of the pulse, respectively (use the `V`, `VV`, `^`, and `^^` buttons to move up and down in the parameter list). When the amplitude is positive, this corresponds to a **depolarizing** pulse, i.e., one that tends to make V become more positive. (Be careful: This convention as to sign of stimulus current is reversed in some papers!) Conversely, a negative `amplitude` corresponds to a **hyperpolarizing** pulse.

Change `amplitude` to 10. Make an integration run by clicking on `Go` in this window.

You will see a nice action potential, showing that the stimulus pulse is **suprathreshold**.

Decrease `amplitude` to 5, rerun the integration, and notice the subthreshold response of the membrane (change the scale on the y -axis to see better if necessary, using `Viewaxes` from the main `XPP` window). The damped oscillatory response of the membrane is a clue to the type of fixed point present. Is it a node? a saddle? a focus? (see Chapter 2).

Compute the eigenvalues of the fixed point by selecting `Sing Pts` from the main `XPP` window, then `Go`, and clicking on `YES` in response to `Print eigenvalues?` Since the system is four-dimensional, there are four eigenvalues. In this instance, there are two real eigenvalues and one complex-conjugate pair. What is the significance of the fact that all eigenvalues have negative real part? Does this calculation of the eigenvalues confirm your guess above as to the nature of the fixed point? Do the numerical values of the eigenvalues (printed in the main window from which `XPP` was originally invoked) tell you anything about the frequency of the damped subthreshold oscillation observed earlier (see Chapter 2)? Estimate the period of the damped oscillation from the eigenvalues.

Let us now investigate the effect of changing a parameter in the equations.

Click on **curbias** in **Parameters** and change its value to -7 . This change now corresponds to injecting a constant **hyperpolarizing** current of $7 \mu\text{A}/\text{cm}^2$ into the membrane (see Chapter 4).

Run the integration and resize the plot window if necessary using **Viewaxes**.

After a short transient at the beginning of the trace, one can see that the membrane is now resting at a more hyperpolarized potential than its original resting potential of -60 mV .

How would you describe the change in the qualitative nature of the subthreshold response to the current pulse delivered at $t = 20 \text{ ms}$?

Use **Sing Pts** to recalculate the eigenvalues and see how this supports your answer.

Let us now see the effect of injecting a constant **depolarizing** current.

Change **curbias** to 5, and make an integration run.

The membrane is now, of course, resting, depolarized to its usual value of -60 mV .

What do you notice about the damped response following the delivery of the current pulse?

Obtain the eigenvalues of the fixed point.

Try to understand how the change in the numerical values of the complex pair explains what you have just seen in the voltage trace.

- (b) **Single-Pulse Triggering.** Now set **curbias** to 10 and remove the stimulus pulse by setting **amplitude** to zero. Carry out an integration run. You should see a dramatic change in the voltage waveform. What has happened?

Recall that n is one of the four variables in the Hodgkin-Huxley equations. Plot out the trajectory in the (Vn) -plane: Click on **Viewaxes** in the main XPP window and then on 2D; then enter **X-axis:V**, **Y-axis:n**, **Xmin:-80**, **Ymin:0.3**, **Xmax:40**, **Ymax:0.8**.

You will see that the limit cycle (or, more correctly, the projection of it onto the (Vn) -plane) is asymptotically approached by the trajectory. If we had chosen as our initial conditions a point exactly on the limit cycle, there would have been no such transient present. You might wish to examine the projection

of the trajectory onto other two-variable planes or view it in a three-dimensional plot (using `Viewaxes` and then `3D`, change the `Z-axis` variable to h , and enter 0 for `Zmin` and 1 for `Zmax`). Do not be disturbed by the mess that now appears! Click on `Window/Zoom` from the main `XPP` window and then on `Fit`. A nice three-dimensional projection of the limit-cycle appears.

Let us check to see whether anything has happened to the fixed point by our changing `curbias` to 10. Click on `Sing pts, Go`, and then `YES`.

`XPP` confirms that a fixed point is still present, and moreover, that it is still stable.

Therefore, if we carry out a numerical integration run with initial conditions close enough to this fixed point, the trajectory should approach it asymptotically in time.

To do this, click on `Erase` in the main `XPP` window, enter the equilibrium values of the variables V, m, h, n as displayed in the bottom of the `Equilibria` window into the `Initial Data` menu, and carry out an integration run.

You will probably not notice a tiny point of light that has appeared in the 3D plot. To make this more transparent, go back and plot V vs. t , using `Viewaxes` and `2D`.

Our calculation of the eigenvalues of the fixed point and our numerical integration runs above show that the fixed point is stable at a depolarizing bias current of $10 \mu\text{A}/\text{cm}^2$. However, remember that our use of the word stable really means **locally** stable; i.e., initial conditions in a sufficiently small neighborhood around the fixed point will approach it. In fact, our simulations already indicate that this point cannot be globally stable, since there are initial conditions that lead to a limit cycle. One can show this by injecting a current pulse.

Change `amplitude` from zero to 10, and run a simulation. The result is the startup of spontaneous activity when the stimulus pulse is injected at $t = 20$ ms (“**single-pulse triggering**”). Contrast with the earlier situation with no bias current injected.

- (c) **Annihilation.** The converse of single-pulse triggering is **annihilation**. Starting on the limit cycle, it should be possible to terminate spontaneous activity by injecting a stimulus that would put the state point into the basin of attraction of the fixed point. However, one must choose a correct combination of stimulus “strength” (i.e., amplitude and duration) and timing. Search for and find a correct combination (Figure 3.20 will give you a hint as to what combination to use).

- (d) **Supercritical Hopf Bifurcation.** We have seen that injecting a depolarizing bias current of $10 \mu\text{A}/\text{cm}^2$ allows annihilation and single-pulse triggering to be seen.

Let us see what happens as this current is increased.

Put `amplitude` to zero and make repeated simulation runs, changing `curbias` in steps of 20 starting at 20 and going up to $200 \mu\text{A}/\text{cm}^2$.

What happens to the spontaneous activity? Is there a bifurcation involved?

Pick one value of bias current in the range just investigated where there is no spontaneous activity.

Find the fixed point and determine its stability using `Sing pts`. Will it be possible to trigger into existence spontaneous activity at this particular value of bias current?

Conduct a simulation (i.e., a numerical integration run) to back up your conclusion.

- (e) **Auto at Last!** It is clear from the numerical work thus far that there appears to be no limit-cycle oscillation present for bias current sufficiently small or sufficiently large, but that there is a stable limit cycle present over some intermediate range of bias current (our simulations so far would suggest somewhere between 10 and $160 \mu\text{A}/\text{cm}^2$). It would be very tedious to probe this range finely by carrying out integration runs at many values of the parameter `curbias`, and in addition injecting pulses of various amplitudes and polarities in an attempt to trigger or annihilate activity. The thing to do here is to run `Auto`, man!

Open `Auto` by selecting `File` and then `Auto` from the main `XPP` window. This opens the main `Auto` window (*It's Auto man!*). Select the `Parameter` option in this window and replace the default choice of `Par1 (blockna)` by `curbias`. In the `Axes` window in the main `Auto` menu, select `hI-1o`, and then, in the resulting `AutoPlot` window, change `Xmin` and `Ymin` to 0 and -80 , respectively, and `Xmax` and `Ymax` to 200 and 20, respectively.

These parameters control the length of the x - and y -axes of the bifurcation diagram, with the former corresponding to the bifurcation variable (bias current), and the latter to one of the four possible bifurcation variables V, m, n, h (we have chosen V).

Invoke `Numerics` from the main `Auto` window, change `Par Max` to 200 (this parameter, together with `Par Min`, which is set to zero, sets the range of the bifurcation variable (`curbias`) that will be investigated).

Also change `Nmax`, which gives the maximum number of points

that **Auto** will compute along one bifurcation branch before stopping, to 500.

Also set **NPr** to 500 to avoid having a lot of labeled points. Set **Norm Max** to 150.

Leave the other parameters unchanged and return to the main **Auto** window.

Click on the main **XPP** window (*not* the main **Auto** window), select **ICs** to bring up the **Initial Data** window, and click on **default** to restore our original initial conditions (V, m, h , and n equal to $-59.996, 0.052955, 0.59599$, and 0.31773 , respectively). Also click on **default** in the **Parameters** window. Make an integration run.

Click on **Run** in the main **Auto** window (**It's Auto man!**) and then on **Steady State**. A branch of the bifurcation diagram appears, with the numerical labels 1 to 4 identifying points of interest on the diagram. In this case, the point with label **LAB** = 1 is an endpoint (EP), since it is the starting point; the points with **LAB** = 2 and **LAB** = 3 are Hopf-bifurcation points (HB), and the point with **LAB** = 4 is the endpoint of this branch of the bifurcation diagram (the branch ended since **Par Max** was attained). The points lying on the parts of the branch between **LAB** = 1 and 2 and between 3 and 4 are plotted as thick lines, since they correspond to stable fixed points. The part of the curve between 2 and 3 is plotted as a thin line, indicating that the fixed point is unstable.

Click on **Grab** in the main **Auto** window. A new line of information will appear along the bottom of the main **Auto** window. Using the \rightarrow key, move sequentially through the points on the bifurcation diagram. Verify that the eigenvalues (plotted in the lower left-hand corner of the main **Auto** window) all lie within the unit circle for the first 47 points of the bifurcation diagram. At point 48 a pair of eigenvalues crosses through the unit circle, indicating that a Hopf bifurcation has occurred. A transformation has been applied to the eigenvalues here, so that eigenvalues in the left-hand complex plane (i.e., those with negative real part) now lie within the unit circle, while those with positive real part lie outside the unit circle.

Let us now follow the limit cycle created at the Hopf bifurcation point (Pt = 47, LAB = 2), which occurs at a bias current of $18.56 \mu\text{A}/\text{cm}^2$. Select this point with the \rightarrow and \leftarrow keys. Then press the **<Enter>** key and click on **Run**. Note that the menu has changed. Click on **Periodic**. You will see a series of points

(the second branch of the bifurcation diagram) gradually being computed and then displayed as circles.

The open circles indicate an unstable limit cycle, while the filled circles indicate a stable limit cycle. The set of circles lying above the branch of fixed points gives the maximum of V on the periodic orbit at each value of the bias current, while the set of points below the branch of fixed points gives the minimum. The point with $LAB = 5$ at a bias current of $8.03 \mu\text{A}/\text{cm}^2$ is a limit point (LP) where there is a saddle-node bifurcation of periodic orbits (see Chapter 3).

Are the Hopf bifurcations sub- or supercritical (see Chapter 2)?

For the periodic branch of the bifurcation diagram, the Floquet multipliers are plotted in the lower left-hand corner of the screen. You can examine them by using **Grab** (use the **<Tab>** key to move quickly between labeled points). Note that for the stable limit cycle, all of the nontrivial multipliers lie within the unit circle, while for the unstable cycle, there is one that lies outside the unit circle. At the saddle-node bifurcation of periodic orbits, you should verify that this multiplier passes through $+1$ (see Chapter 3).

After all of this hard work, you may wish to keep a PostScript copy of the bifurcation diagram (using **file** and **Postscript** from the main **Auto** window). You can also keep a working copy of the bifurcation diagram as a diskfile for possible future explorations (using **File** and **Save diagram**). Most importantly, you should sit down for a few minutes and make sure that you understand how the bifurcation diagram computed by **Auto** explains all of the phenomenology that you obtained from the pre-**Auto** (i.e., numerical integration) part of the exercise.

- (f) **Other Hodgkin–Huxley Bifurcation Parameters.** There are many parameters in the Hodgkin–Huxley equations. You might try constructing bifurcation diagrams for any one of these parameters. The obvious ones to try are *gna*, *gk*, *gleak*, *ena*, *ek*, and *leak* (see equation (4.25)).
- (g) **Critical Slowing Down.** When a system is close to a saddle-node bifurcation of periodic orbits, the trajectory can spend an arbitrarily long time traversing the region in a neighborhood of where the semistable limit cycle will become established at the bifurcation point. Try to find evidence of this in the system studied here.

Ex. 4.7-2. **Two Stable Resting Potentials in the Hodgkin–Huxley Equations.** Under certain conditions, axons can demonstrate two stable resting potentials (see Figure 3.1 of Chapter 3). We will compute the bifurcation diagram of the fixed points using the modified Hodgkin–Huxley equations in the XPP file **hh2sss.ode**. The bifurcation parameter is now the external potassium concentration **kout**.

- (a) **Plotting the bifurcation diagram.** This time, let us invoke **Auto** as directly as possible, without doing a lot of preliminary numerical integration runs.

Make a first integration run using the source file **hh2sss.ode**. The transient at the beginning of the trace is due to the fact that the initial conditions correspond to a bias current of zero, and we are presently injecting a hyperpolarizing bias current of $-18 \mu\text{A}/\text{cm}^2$.

Make a second integration run using as initial conditions the values at the end of the last run by clicking on **Initialconds** and then **Last**. We must do this, since we want to invoke **Auto**, which needs a fixed point to get going with the continuation procedure used to generate a branch of the bifurcation diagram. Start up the main **Auto** window. In the **Parameter** window enter **kout** for **Par1**. In the **Axes** window, enter 10, -100 , 400, and 50 for **Xmin**, **Ymin**, **Xmax**, and **Ymax**, respectively. Click on **Numerics** to obtain the **AutoNum** window, and set **Nmax:2000**, **NPr:2000**, **Par Min:10**, **Par Max:400**, and **Norm Max:150**. Start the computation of the bifurcation diagram by clicking on **Run** and **Steady state**.

- (b) **Studying points of interest on the bifurcation diagram.** The point with label **LAB = 1** is an endpoint (EP), since it is the starting point; the points with **LAB = 2** and **LAB = 3** are limit points (LP), which are points such as saddle-node and saddle-saddle bifurcations, where a real eigenvalue passes through zero (see Chapter 3).

The point with **LAB = 4** is a Hopf-bifurcation (HB) point that we will study further later. The endpoint of this branch of the bifurcation diagram is the point with **LAB = 5** (the branch ended since **Par Max** was attained).

The points lying on the parts of the branch between **LAB = 1** and **2** and between **4** and **5** are plotted as thick lines, since they correspond to stable fixed points. The parts of the curve between **2** and **3** and between **3** and **4** are plotted as thin lines, indicating that the fixed points are unstable.

Note that there is a range of **kout** over which there are two sta-

ble fixed points (between the points labeled 4 and 2).

Let us now inspect the points on the curve.

Click on **Grab**.

Verify that the eigenvalues all lie within the unit circle for the first 580 points of the bifurcation diagram. In fact, all eigenvalues are real, and so the point is a stable node.

At point 580 ($\text{LAB} = 2$) a single real eigenvalue crosses through the unit circle at $+1$, indicating that a limit point or turning point has occurred. In this case, there is a saddle-node bifurcation of fixed points.

Between points 581 and 1086 ($\text{LAB} = 2$ and 3 respectively), there is a saddle point with one positive eigenvalue. The stable manifold of that point is thus of dimension three, and separates the four-dimensional phase space into two disjoint halves.

At point 1086 ($\text{LAB} = 3$), a second eigenvalue crosses through the unit circle at $+1$, producing a saddle point whose stable manifold, being two-dimensional, no longer divides the four-dimensional phase space into two halves. The two real positive eigenvalues collide and coalesce somewhere between points 1088 and 1089, then split into a complex-conjugate pair.

Both of the eigenvalues of this complex pair cross and enter the unit circle at point 1129 ($\text{LAB} = 4$). Thus, the fixed point becomes stable. A reverse Hopf bifurcation has occurred, since the eigenvalue pair is purely imaginary at this point (see Chapter 2). Press the **<Esc>** key to exit from the **Grab** function.

Keep a copy of the bifurcation diagram on file by clicking on **File** and **Save Diagram** and giving it the filename **hh2sss.ode.auto**.

- (c) **Following Periodic Orbit Emanating from Hopf Bifurcation Point.** A Hopf bifurcation (HB) point has been found by **Auto** at point 1129 ($\text{LAB} = 4$). Let us now generate the periodic branch emanating from this HB point.

Load the bifurcation diagram just computed by clicking on **File** and then on **Load diagram** in the main **Auto** window. The bifurcation diagram will appear in the plot window.

Reduce **Nmax** to 200 in **Numerics**, select the HB point ($\text{LAB} = 4$) on the diagram, and generate the periodic branch by clicking on **Run** and then **Periodic**.

How does the periodic branch terminate? What sort of bifurca-

tion is involved (see Chapter 3)?

Plotting the period of the orbit will help you in figuring this out. Do this by clicking on **Axes** and then on **Period**. Enter 50, 0, 75, and 200 for **Xmin**, **Ymin**, **Xmax**, and **Ymax**.

- (d) **Testing the results obtained in Auto.** Return to the main **XPP** menu and, using direct numerical integration, try to see whether the predictions made above by **Auto** (e.g., existence of two stable resting potentials) are in fact true. Compare your results with those obtained in the original study (Aihara and Matsumoto 1983) on this problem (see e.g., Figure 3.7).

Ex. 4.7-3. Reduction to a Three-Dimensional System. It is difficult to visualize what is happening in a four-dimensional system. The best that the majority of us poor mortals can handle is a three-dimensional system. It turns out that much of the phenomenology described above will be seen by making an approximation that reduces the dimension of the equations from four to three. This involves removing the time-dependence of the variable m , making it depend only on voltage.

Exit **XPP** and copy the file **hh.ode** to a new file **hhminf.ode**. Then edit the file **hhminf.ode** so that m^3 is replaced by m_∞^3 in the code for the equation for **curna**: That is, replace the line,

```
curna(v) = blockna*gna*m^3*h*(v-ena)
```

with

```
curna(v) = blockna*gna*minf(v)^3*h*(v-ena)
```

Run **XPP** on the source file **hhminf.ode** and view trajectories in 3D.

4.8 Computer Exercises: A Numerical Study on the FitzHugh–Nagumo Equations

In these computer exercises, we carry out numerical integration of the FitzHugh–Nagumo equations, which are a two-dimensional system of ordinary differential equations.

The objectives of the first exercise below are to examine the effect of changing initial conditions on the time series of the two variables and on the phase-plane trajectories, to examine nullclines and the direction field in the phase-plane, to locate the stable fixed point graphically and numerically, to determine the eigenvalues of the fixed point, and to explore the concept of excitability. The remaining exercises explore a variety of phenomena characteristic of an excitable system, using the FitzHugh–Nagumo equations

as a prototype (e.g., refractoriness, anodal break excitation, recovery of latency and action potential duration, strength–duration curve, the response to periodic stimulation). While detailed keystroke-by-keystroke instructions are given for the first exercise, detailed instructions are not given for the rest of the exercises, which are of a more exploratory nature.

The FitzHugh–Nagumo Equations

We shall numerically integrate a simple two-dimensional system of ordinary differential equations, the FitzHugh–Nagumo equations (FitzHugh 1961). As described earlier on in this chapter, FitzHugh developed these equations as a simplification of the much more complicated-looking four-dimensional Hodgkin–Huxley equations (Hodgkin and Huxley 1952) that describe electrical activity in the membrane of the axon of the giant squid. They have now become the prototypical example of an excitable system, and have been used as such by physiologists, chemists, physicists, mathematicians, and other sorts studying everything from reentrant arrhythmia in the heart to controlling chaos. The FitzHugh–Nagumo equations are discussed in Section 4.5.6 in this chapter and given in equation (4.27). (See also Kaplan and Glass 1995, pp. 245–248, for more discussion on the FitzHugh–Nagumo equations.)

The file **fhn.ode** is the XPP file[†] containing the FitzHugh–Nagumo equations, the initial conditions, and some plotting and integrating instructions for XPP. Start up XPP using the source file **fhn.ode**.

Ex. 4.8-1. Numerical Study of the FitzHugh–Nagumo equations.

- (a) **Time Series.** Start a numerical integration run by clicking on **Initialconds** and then **Go**. You will see a plot of the variable x as a function of time.

Notice that x asymptotically approaches its equilibrium value of about 1.2.

Examine the transient at the start of the trace: Using **Viewaxes** and **2D**, change the ranges of the axes by entering 0 for **Xmin**, 0 for **Ymin**, 10 for **Xmax**, 2.5 for **Ymax**. You will see that the range of t is now from 0 to 10 on the plot.

Now let us look at what the other variable, y , is doing. Click on **Xi vs t** and enter y in the box that appears at the top of the XPP window. You will note that when y is plotted as a function of t , y is monotonically approaching its steady-state value

[†]See Introduction to XPP in Appendix A.

of about -0.6 .

We thus know that there is a stable fixed point in the system at $(x, y) \approx (1.2, -0.6)$. You will be able to confirm this by doing a bit of simple algebra with equation (4.27).

- (b) **Effect of Changing Initial Conditions.** The question now arises as to whether this is the only stable fixed point present in the system. Using numerical integration, one can search for multiple fixed points by investigating what happens as the initial condition is changed in a systematic manner.

Go back and replot x as a function of t .

Rescale the axes to 0 to 20 for t and 0 to 2.5 for x .

Click on the **ICs** button at the top of the **XPP** window. You will see that x and y have initial conditions set to 2, as set up in the file **fn.ode**. Replace the the initial condition on x by -1.0 .

When you integrate again, you will see a second trace appear on the screen that eventually approaches the same asymptotic or steady-state value as before.

Continue to modify the initial conditions until you have convinced yourself that there is only one fixed point in the system of equation (4.27).

Note: Remember that if the plot window gets too cluttered with traces, you can erase them (**Erase** in main **XPP** window).

You might also wish to verify that the variable y is also approaching the same value as before (≈ -0.6) when the initial conditions on x and y are changed.

Reset the initial conditions to their default values.

In finding the equilibria (by using **Sing pts** in **XPP**), you will see that the fixed point is stable and lies at $(x^*, y^*) = (1.1994, -0.62426)$.

While **XPP** uses numerical methods to find the roots of $dx/dt = 0$ and $dy/dt = 0$ in equation (4.27), you can very easily verify this from equation (4.27) with a bit of elementary algebra.

- (c) **Trajectory in the (xy) phase plane.** We have examined the time series for x and y . Let us now look at the trajectories in the (xy) phase plane.

Change the axis settings to to **X-axis:x**, **Y-axis:y**, **Xmin:-2.5**, **Ymin:-2.5**, **Xmax:2.5**, **Ymax:2.5**, and make another integration run. The path followed by the state-point of the system (the

trajectory) will then be displayed.

The computation might proceed too quickly for you to see the direction of movement of the trajectory: However, you can figure this out, since you know the initial condition and the location of the fixed point.

Try several different initial conditions (we suggest the (x, y) pairs $(-1, -1)$, $(-1, 2)$, $(1, -1)$, $(1, 1.5)$).

An easy way to set initial conditions is to use the **Mouse** key in the **Initialconds** menu.

You have probably already noticed that by changing initial conditions, the trajectory takes very different paths back to the fixed point.

To make this clear graphically, carry out simulations with the trajectory starting from an initial condition of $(x_0, y_0) = (1.0, -0.8)$ and then from $(1.0, -0.9)$. In fact, it is instructive to plot several trajectories starting on a line of initial conditions at $x = 1$ (using **Initialconds** and then **Range**) with y changing in steps of 0.1 between $y = -1.5$ and $y = 0$. Note that there is a critical range of y_0 , in that for $y_0 > -0.8$, the trajectory takes a very short route to the fixed point, while for $y_0 < -0.9$, it takes a much longer route.

Use **Flow** in the **Dir.field/flow** menu to explore initial conditions in a systematic way. What kind of fixed point is present (e.g., node, focus, saddle)?

- (d) **Nullclines and the Direction Field.** The above results show that a small change in initial conditions can have a dramatic effect on the resultant evolution of the system (do not confuse this with “sensitive dependence on initial conditions”).

To understand this behavior, draw the nullclines and the direction fields (do this both algebraically and using **XPP**).

What is the sign of dx/dt in the region of the plane above the x -nullcline? below the x -nullcline? How about for the y -nullcline? You can figure this out from equation (4.27), or let **XPP** do it for you.

By examining this **direction field** (the collection of tangent vectors), you should be able to understand why trajectories have the shape that they do.

Try running a few integrations from different initial conditions set with the mouse, so that you have a few trajectories superimposed on the vector field.

- (e) **Excitability.** The fact that small changes in initial conditions can have a large effect on the resultant trajectory is responsible for the property of **excitability** possessed by the FitzHugh–

Nagumo equations. Let us look at this directly.

Click on **Viewaxes** and then **2D**. Set **X-axis:t**, **Y-axis:x**, **Xmin:0.0**, **Ymin:-2.5**, **Xmax:20.0**, **Ymax:2.5**. Set $x = 1.1994$ and $y = -0.62426$ as the new initial conditions and start an integration run.

The trace is a horizontal line, since our initial conditions are now at the fixed point itself: the transient previously present has evaporated. Let us now inject a stimulus pulse.

In the **Param(eter)** window, enter

amplitude=-2.0, **tstart=5.0**, and **duration=0.2**.

We are thus now set up to inject a depolarizing stimulus pulse of amplitude 2.0 and duration 0.2 time units at $t = 5.0$. We shall look at the trace of the auxiliary variable v , which was defined to be equal to $-x$ in **fhn.ode**. We need to look at $-x$, since we will now identify v with the transmembrane potential.

Using **Xi vs t** to plot v vs. t , you will see a “voltage waveform” very reminiscent of that recorded experimentally from an excitable cell, i.e., there is an action potential with a fast upstroke phase, followed by a phase of repolarization, and a hyperpolarizing afterpotential.

Change the pulse amplitude to -1.0 and run a simulation. The response is now subthreshold.

Make a phase-plane plot (with the nullclines) of the variables x and y for both the sub- and suprathreshold responses, to try to explain these two responses.

Explore the range of amplitude between 0.0 and -2.0 . The concept of an effective “threshold” should become clear.

Calculate the eigenvalues of the fixed point using the **Sing pts** menu. The eigenvalues appear in the window from which **XPP** was invoked.

Does the nature of the eigenvalues agree with the fact that the subthreshold response resembled a damped oscillation?

Predict the period of the damped oscillation from the eigenvalues and compare it with what was actually seen.

- (f) **Refractoriness.** Modify the file **fhn.ode** so as to allow two successive suprathreshold stimulus pulses to be given (it might be wise to make a backup copy of the original file). Investigate how the response to the second stimulus pulse changes as the interval between the two pulses (the coupling interval) is changed. The Heaviside step-function $\text{heav}(t - t_0)$, which is available in **XPP**, is 0 for $t < t_0$ and 1 for $t > t_0$. Is there a coupling interval below which one does not get an action potential?

- (g) **Latency.** The latency (time from onset of stimulus pulse to upstroke of action potential) increases as the interval between two pulses is decreased. Plot latency as a function of coupling interval. Why does the latency increase with a decrease in the coupling interval?
- (h) **Action Potential Duration.** The action potential duration (time between depolarization and repolarization of the action potential) decreases as the coupling interval decreases. Why is this so?
- (i) **Strength–Duration Curve: Rheobase and Chronaxie.** It is known from the earliest days of neurophysiology that a pulse of shorter duration must be of higher amplitude to produce a suprathreshold response of the membrane. Plot the threshold pulse amplitude as a function of pulse duration. Try to explain why this curve has the shape that it has. The minimum amplitude needed to provoke an action potential is termed the *rheobase*, while the shortest possible pulse duration that can elicit an action potential is called *chronaxie*.
- (j) **Anodal Break Response.** Inject a hyperpolarizing pulse (i.e., one with a positive amplitude). Start with a pulse amplitude of 5 and increase in increments of 5. Can you explain why an action potential can be produced by a hyperpolarizing stimulus (“anodal break response”)?
- (k) **Response to Periodic Stimulation.** Investigate the various rhythms seen in response to periodic stimulation with a train of stimulus pulses delivered at different stimulation frequencies. The response of the FitzHugh–Nagumo equations to a periodic input is very complicated, and has not yet been completely characterized.
- (l) **Automaticity.** Another basic property of many excitable tissues is automaticity: the ability to spontaneously generate action potentials. Set $a = 0$ and $t_{\max} = 50$ (click on **Numerics** and then **Total**) and run `fhn.ode`. What has changing the parameter a done? What is the attractor now? What has happened to the stability of the fixed point? What kind of bifurcation is involved? Changing a systematically in the range from 0 to 2 might assist you in answering these questions. How does the shape of the limit cycle change as a is changed?
- (m) **Phase-Locking.** Explore the response of the FitzHugh–Nagumo oscillator to periodic stimulation with a periodic train of current pulses. Systematically change the frequency and amplitude of the pulse train. In another exercise (Section 5.9), phase-locking is studied in an oscillator that is simple enough to allow reduction of the dynamics to consideration of a one-dimensional map. What is the dimension of the map that would result from re-

duction of the FitzHugh–Nagumo case to a map? Can you find instances where the response of the FitzHugh–Nagumo oscillator is different from that of the simpler oscillator?

Ex. 4.8-2. **Two Stable Fixed Points in the FitzHugh–Nagumo Equations.** In the standard version of the FitzHugh–Nagumo equations, there is only one fixed point present in the phase-space of the system.

Since the x -isocline is cubic, the possibility exists for there to be three fixed points in the FitzHugh–Nagumo equations.

Try to find combinations of the parameters a , b , and c such that two stable fixed points coexist (“bistability”).

How would you have to change the FitzHugh–Nagumo equations to obtain more than two stable fixed points (i.e., multistability)?